CHEMISTRY
A European Journal

A Journal of
ChemPubSoc Europe

Accepted Article

Title: A new photocage derived from fluorene

Authors: Matiss Reinfelds, Jan von Cosel, Konstantin Falahati, Carsten Hamerla, Tomas Slanina, Alexander Heckel, and Irene Burghardt

To be cited as: *Chem. Eur. J.* 10.1002/chem.201802390

Link to VoR: http://dx.doi.org/10.1002/chem.201802390

Supported by
ACES

WILEY-VCH

10.1002/chem.201802390

WILEY-VCH

FULL PAPER

A new photocage derived from fluorene

Matiss Reinfelds[†][a], Jan von Cosel[†][b], Konstantin Falahati[b], Carsten Hamerla[b], Tomáš Slanina[a], Irene Burghardt*[b] and Alexander Heckel*[a]

Abstract: Photolabile protecting groups (PPGs or photocages) are increasingly subject to molecular design to meet requirements like absorbance in the visible spectral range, high molar absorption coefficients, and high quantum yields of leaving group release. We report on improvements of these properties for the promising DEAMb (3-diethylaminobenzyl) photocage whose photoactivity is based on Zimmerman`s meta effect. The expansion of the aromatic system with a second aromatic ring resulted in improved spectral properties. A systematic trend relating the new aryl substituent's electronic (π-donor or acceptor) properties and its position in the DEAMb ring, to changes in the spectral properties, could be recognized. Conclusions from the experimental results were supported by computations using Time-Dependent Density Functional Theory (TDDFT). A second generation of DEAMb-based photocages was designed. A rigid linker was introduced to ensure more efficient conjugation of the aromatic ring π-systems by limiting rotational freedom. The resulting fluorenol (9-hydroxyfluorene) based photocages had superior spectral properties compared to the simple biphenyl systems. The best uncaging cross section achieved was 5320 M^{-1} cm^{-1} ($\varepsilon\Phi_{365}$).

Introduction

The use of photolabile protecting groups (PPGs or photocages) for temporarily blocking biologically active molecules was pioneered by Engels[1] and Kaplan.[2] Since then photocages have proven useful tools for various biological applications.[3,4] Recent examples include local activation of antimiR-92a in living mice, which improves wound healing,[5] manipulation of a protein function in living zebrafish embryos[6] and induction of calcium signaling events in mouse cardiac myocytes.[7] In order to utilize biologically acceptable and penetrable irradiation for complex scenarios of light control, further development of efficient, visible light absorbing photocages is desired. This motivated the systematic redshifting of the absorbance spectra of known photocages, such as *o*-nitrobenzyl,[8] *o*-hydroxycinnamyl[9,10] and coumarin.[11–14] Also new visible light activatable PPGs have been published recently, for example, pyridinium esters,[15] trimethyl lock,[16] and heptamethine cyanine-based photocages.[17] However, the troublesome optimization of the chromophore structure and substitution is still the major problem in the PPG development, since a relatively small change can greatly influence the photoactivity. Computational methods can be used as a tool for rational design of PPGs.[18] Guided by simple Hückel MO predictions, Wirz, Klán and their coworkers were the first to report a new photocage based on visible light absorbing fluorophores.[19] Since then, promising new PPGs have been developed based on the BODIPY fluorophore.[20–24] However, BODIPY photocages so far are limited to direct release of a good leaving group (LG). In–contrast, Wang has demonstrated the remarkable power of the simple 3-diethylamino benzyl (DEAMb, **1**, see Scheme 1) chromophore for the release of poor leaving groups, such as amines[25] and alcohols.[26] This photocage based on Zimmerman's meta effect[27] and its analogues have been reviewed in a detailed account.[28] The main drawback of this chromophore is the need of using UV light (<350 nm) for excitation. The promising reactivity of DEAMb motivated us to explore the possibility of shifting its absorption to longer wavelengths by combining computational predictions with synthesis.

Results and Discussion

Synthesis of the biphenyl compounds:

In order to optimize the structure of the DEAMb photocage, we spatially extended the π-orbital conjugation. Thus, an aryl substituent was installed by Suzuki coupling to various positions of DEAMb. To this end, DEAMb-derived halide precursors for the Suzuki coupling reaction were prepared (**P1**, Scheme 1) and L-glutamic acid was attached as a leaving group (**P2**). Esters are often chosen as test systems due to the ease of installation and the non-nucleophilic nature of the departing carboxylate anion. After a cross-coupling reaction (→**P3**) the protecting groups of the glutamic acid side chain were cleaved by trifluoroacetic acid to give the desired biaryls (**2-5)**. The cross-coupling reaction was always slower for *ortho* isomers (relative to the NEt_2 group), likely due to the steric hindrance. Particularly bad reactivity was observed for the isomer where the halogen atom is located between the other two substituents of the aromatic ring (**5**). Prolonged reaction time did not lead to higher reaction yields due to side reactions, such as hydrodehalogenation of starting material.[29] Hydrolysis of the coupling products **P3** could also be observed if the reaction was stirred for a longer time. Boronic acid homocoupling always happened to some extent and the produced symmetric biaryls could not be easily separated by normal phase column chromatography from the

[a] M. Reinfelds, Dr. T. Slanina, Prof. Dr. A.Heckel
Institute of Organic Chemistry and Chemical Biology
Goethe University Frankfurt
Max-von-Laue-Str. 7, 60438 Frankfurt, Germany.
E-mail: heckel@uni-frankfurt.de
[b] J. von Cosel, K. Falahati, C. Hamerla, Prof. Dr. Irene Burghardt
Institute of Physical and Theoretical Chemistry
Goethe University Frankfurt
Max-von-Laue-Str. 7, 60438 Frankfurt, Germany.
E-mail: burghardt@chemie.uni-frankfurt.de
[†] These authors contributed equally to this work

Supporting information for this article is given via a link at the end of the document

10.1002/chem.201802390

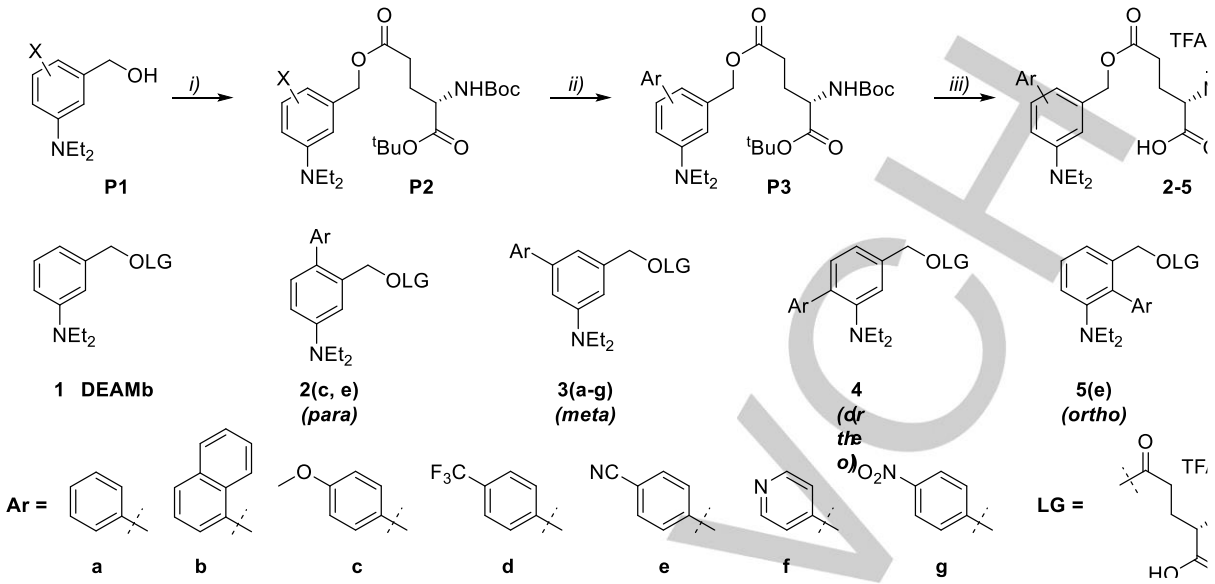

Scheme 1. First row: reaction sequence for the synthesis of glutamic acids biphenyl esters: *i*) Boc-Glu-O^{t}Bu, EDC-HCl, DMAP, DIPEA, CH_2Cl_2, r.t. overnight *ii*) Ar-$B(OH)_2$, $Pd(PPh_3)_4$, Na_2CO_3, toluene/EtOH/H_2O, 110 °C, 5-12 h; *iii*) TFA, CH_2Cl_2, r.t., overnight; X = halogen; Second row: the structures of the synthesised biphenyl derivatives (letters in parentheses indicate which of the substituent combinations were prepared).

desired product due to their similar structures. Separation was easy, though, by reverse phase (C18) chromatography, especially if done after cleavage of Boc and ^{t}Bu esters.

Photochemical characterisation of the biphenyl compounds

We first explored donor-acceptor (D-π-A) systems, which are known to bathochromically shift the absorbance spectrum and increase the molar absorption coefficients.[30] The 4-CN phenyl

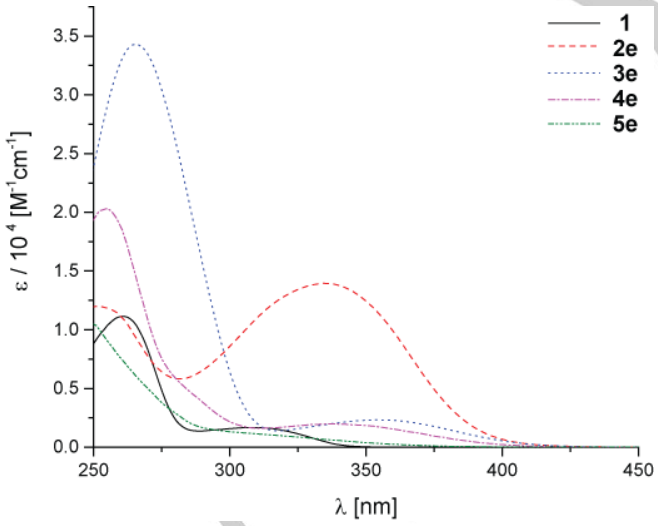

Figure 1. Molar absorption coefficients of DEAMb (**1**) and its derivatives bearing a *p*-NC-C_6H_4- substituent in *para* (**2e**), *meta* (**3e**) and *ortho* (**4e**, **5e**) positions (in 0.1M TEAA buffer with 20% MeCN).

substituent (Ar = **e**, Scheme 1) was installed in various positions of the aromatic ring. The *para* substituted molecule (**2e**) shows a prominent charge transfer (CT) band with λ_{max} at 335 nm (Figure 1). Although the S_0-S_1 absorbance maximum of the regioisomers **3e** (355 nm) and **4e** (338 nm) are slightly more bathochromically shifted as compared to **2e** (Table 1), the molar absorption coefficients are about five times smaller since there is a less pronounced *push-pull* character between electron donor and acceptor. Nevertheless, all three isomers show improvements when compared to unsubstituted DEAMb (**1**). The smallest molar absorption coefficient in the whole wavelength range was obtained with molecule **5e**. This is attributed to a large steric hindrance of the substituent in both *ortho* positions of the biphenyl bond. As a result, the phenyl rings are twisted out of co-planarity, thereby limiting the π orbitals overlap.[31] The quantum yields of starting material disappearance were measured at 365 nm and are shown in Table 1. Unfortunately, the spectroscopically superior isomer **2e** demonstrated a small uncaging quantum yield (Φ_{365} = 0.2%) resulting in a low uncaging cross section (21 M^{-1} cm^{-1}). It is known that intramolecular charge transfer can result in depletion of photoactivity.[32] Similar quantum yield values were also obtained for regioisomers **3e** and **5e** and their uncaging cross sections were even smaller (1 M^{-1} cm^{-1}). The molecule **4e** had the highest quantum yield and the best uncaging cross section at 365 nm (53 M^{-1} cm^{-1}). For the isomers **2e**, **4e** and **5e** the major photoproduct resulting from a photosolvolysis reaction was the corresponding benzyl alcohol, while **3e** gave a mixture of unidentified photoproducts (Fig. S3-5, Supporting Information). The steric hindrance at *ortho* positions (compounds **4** and **5**) makes them unpractical for testing further substituent effects. Instead, we compared the effect of electron accepting and electron donating substituents in *para* (**2**) and *meta* (**3**) positions

10.1002/chem.201802390

by replacing the cyano substituent with the methoxy substituent, creating D-π-D system. The λ_{max} of the newly produced compound **2c** was hypsochromically shifted by 56 nm and it showed no absorbance at wavelengths above 350 nm (Fig. S6, Supporting Information). The longest wavelength absorption band of *meta* isomer **3c** was hypsochromically shifted only by 22 nm (Figure 2).

Table 1. Photochemical properties of DEAMb derivatives bearing *p*-CN-C_6H_4-substituents.

Compd.[a]	λ_{max}[b] (nm)	$\varepsilon_{\lambda max}$[b] ($M^{-1}$ cm^{-1})	ε_{365} (M^{-1} cm^{-1})	Φ_{365} (%)	$\varepsilon\Phi_{365}$[c] (M^{-1} cm^{-1})
1	309	1681	0	12[d]	200[d]
2e	335	13 950	8396	0.25	21
3e	355	2320	2156	0.04	<1
4e	338	1980	1330	4	53
5e	251	10420	205	0.6	1

[a] All measurements were done in 0.1M TEAA buffer with 20% MeCN. [b] The value of the absorbance band at the longest wavelength (S_0-S_1 transition) where it is possible to distinguish. [c] Uncaging cross section. [d] Determined at 310 nm.

The substantial increase of the uncaging quantum yield for molecule **3c** (Φ_{365} = 19%, Table 2) encouraged us to further explore the substituent electronic effects in the *meta* position (**3a-g**) to the absorbance spectrum (Figure 2). The phenyl (**3a**) and naphthyl (**3b**) substituents bathochromically shift the longest wavelength absorbance band of DEAMb (**1**) by more than 20 nm (Table 2) and increase the molar absorption coefficient just like the methoxyphenyl substituent (**3c**). The uncaging quantum yield at 365 nm is better for compound **3a** (42%). Further bathochromic shift can be observed if electron-withdrawing aryl substituents are introduced (**3e-g**).

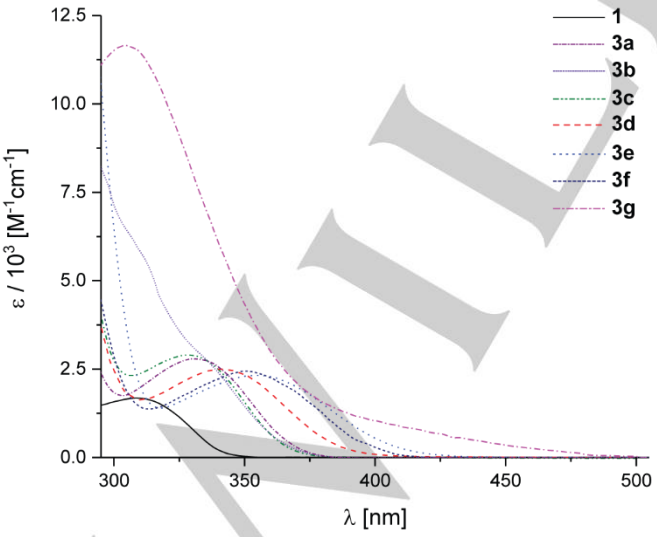

Figure 2. Molar absorption coefficients of DEAMb (**1**) and its derivatives bearing aryl substituents in *meta* position (**3a-g**). All measurement were done in 0.1M TEAA buffer with 20% MeCN.

Yet, improved spectral properties come at the expense of decreasing quantum yield. If a substituent has a relatively weak electron acceptor character, such as *p*-F_3C-C_6H_4 (**3d**), the quantum yield is still fine (Φ_{365} = 5%). However, in the case of *p*-NO_2-C_6H_4 (**3g**) no photoactivity at 365 nm could be seen.

TDDFT computations of biphenyl compounds

The observed reactivity can be rationalized on the basis of Zimmerman´s meta effect. Knowing that DEAMb (**1**) demonstrates photoactivity due to increased electron density in *meta* positions upon excitation, it comes as no surprise that an electron withdrawing group (EWG) in one of the *meta* positions will decrease the photoactivity. This effect was qualitatively confirmed by computational investigations. TDDFT (Time Dependent Density Functional Theory) excited state analysis was performed at the PBE0/Def2-TZVP level of theory using the Gaussian16 program package.[33–35] Ground state structures were optimized and all minima verified by frequency calculations. As can be inferred from Fig. S7 (Supporting Information), the frontier orbitals are modified upon introduction of electron withdrawing or donating groups to the aromatic phenyl scaffold. Systematic increase of local orbital contribution at the benzylic position, where the leaving group is attached, is obtained for **3a** and **3c.** This is in sharp contrast to the nitro substituted compound **3g** for which no corresponding bond pre-labilization tendency could be observed. However, although the introduction of additional substituents leads to a general redshift of the absorption maximum, the electronic structure study remains inconclusive with respect to the choice of the best uncaging candidate given the close electronic kinship of the biphenyl derivatives (again with the notable exception of **3g**). Table 2 displays the relative energetics of the bright state singlet excitations as computed in this study. Near-quantitative agreement with the experimental data is achieved.

Summary for biphenyl compounds

The absorbance of the DEAMb photocage can be redshifted by extending the π-orbital conjugation using biphenyls. Photoactivity is preserved if no strong EWG is used. However, the molar absorption coefficients at 365 nm are rather low because the phenyl rings are twisted out of co-planarity. The release of the glutamic acid from the compound **3a** could be demonstrated indirectly by comparing a standard of the expected photoproduct (benzyl alcohol) with irradiated sample of the compound **3a** (Fig. S8, Supporting Information). Also, direct proof of the glutamic acid release could be shown by ^{1}H NMR spectroscopy (Fig. S9, Supporting Information). Thermal hydrolysis of the biphenyl **3a** in the dark is slow (1% in 10 h). Our best candidates have similar (**3c** Φ_{365} = 19%) or better (**3a** Φ_{365} = 42%) quantum yields of uncaging at 365 nm than the parent DEAMb (**1**) has at higher energy wavelength (Φ_{310} = 12%, Table 2).

Table 2. Photochemical properties of DEAMb derivatives bearing aryl substituents in *meta* position.

Compd.[a]	Ar	λ_{max} S_0-S_1 (nm)[b]	Excitation energy S_0-S_1 (nm)[c]	Oscillator strength[c]	$\varepsilon\lambda_{max}$ S_0-S_1 (M^{-1} cm^{-1})	ε_{365} (M^{-1} cm^{-1})	Φ_{365} (%)	$\varepsilon\Phi_{365}$ (M^{-1} cm^{-1})[d]
1		309	n.d.[e]	n.d.	1681	0	12[f]	200[f]
3a	Ph	331	307	0.0598	2825	535	**42**	**225**
3b	Napth	334	n.d.	n.d.	2860	400	1.9	8
3c	*p*-CH_3O-C_6H_4-	327	299	0.0824	3048	484	19	92
3d	*p*-CF_3-C_6H_4-	340	328	0.0513	2504	1472	4.6	68
3e	*p*-CN-C_6H_4-	355	354	0.0456	2320	2156	0.04	<1
3f	Py	349	n.d.	n.d.	2445	2038	0.01	<1
3g	*p*-NO_2-C_6H_4-	304	308[g]	0.2494[g]	11651	2463	no reaction	-

[a] All measurement were done in 0.1M TEAA buffer with 20% MeCN. [b] The value of the absorbance band at the longest wavelength (S_0-S_1 transition). [c] Corresponding computed excitation energies obtained at the TD-PBE0/Def2-TZVP level of theory. At the amino group ethyl was replaced with methyl, the leaving group replaced with –OH. [d] Uncaging cross section. [e] Not determined. [f] Determined at 310 nm. [g] The S_3 state was assigned to the experimental value in this case.

Reported quantum yields for alcohol release from the DEAMb were 20-26% (medium pressure mercury lamp with Pyrex filter >280 nm).[26,36] Acetate could be released with 8% quantum yield (at 254 nm) from the *meta*-*N*,*N*-dimethylaminobenzyl photocage (DMAMb).[37] Our results and comparison with known data demonstrated that we have successfully shifted the absorbance spectrum of the DEAMb photocage to longer wavelengths without losing its good reactivity. With these promising results in hand, we set out to rationally design the second generation of DEAMb-based photocages with further improvements of its photochemical properties.

Fluorene derivatives as PPGs

Based on the experimental results and computational data, we realized that achieving planarity of the biphenyl derivatives would be favorable. A simple way of blocking the rotational freedom around the biphenyl C-C bond is by linking the DEAMb benzylic carbon to a second aromatic ring (*e.g.*, fluorene) via a single bond. Fluorenol (9-hydroxyfluorene) is known to produce a fluorenyl carbocation upon excitation.[38] In the ground state it is an antiaromatic system (4*n* π electrons) but it is aromatic in the excited state.[39,40] As a result, the fluorenyl carbocation has a low energetic excited state and a high energetic ground state. The corresponding potential energy surfaces are located in close proximity and this can lead to productive photoheterolysis via conical intersection as recently postulated by Winter *et al*.[41] Lukeman and coworkers showed uncaging of 2,7-disubstituted-9-fluorenol acetate by irradiation at 300 nm.[42] Fluorene quaternary ammonium derivatives have also been used as a photobase releasing free tertiary amines.[43] An initial study of the photochemical properties of 2,7-diamino-9-fluorenol has been done in the laboratory of Wirz.[44]

We synthesized the fluorenol derivative **9** (Scheme 2, first line) from the commercially available 2-amino-fluoren-9-one (**6**) by reductive amination (**7**), followed by Steglich-type esterification (**8**) and protecting group cleavage. The molar absorption coefficient of the molecule **9** at the absorbance maximum (λ_{max} = 311 nm) is 24 150 M^{-1} cm^{-1} and 1190 M^{-1} cm^{-1} at 365 nm (Fig. S10, Supporting Information). Upon irradiation, the release of glutamic acid could be observed and the fluorenol alcohol (**7**) was the major photoproduct (Fig. S11 and S12, Supporting Information). The uncaging cross section of 274 M^{-1} cm^{-1} (Φ_{365} = 23%) is slightly better than that of the best biphenyl derivative **3a**. The rate of thermal hydrolysis of compound **9** in the dark is slow (4 x 10^{-11} M s^{-1}) which corresponds for example to 4% thermal uncaging over 10 h under the given experimental conditions (sample concentration 3.4 mol L^{-1} in 0.1M TEAA buffer with 20% MeCN). The expected spectral improvement and good quantum yield encouraged us to further explore the photochemistry of fluorenols.

TDDFT calculations on fluorenol derivatives

To guide our synthetic effort, the potential substituent effects were predicted using TDDFT. A clearly recognisable meta effect, as in the case of DEAMb derived biphenyls, could not be claimed for fluorenol derivatives. We discovered that the excited states mainly consist of two types of electronic transitions. A representative example is shown for compound **10** in Figure 3. The spectroscopically accessible bright state involves an orbital transition of $\pi \rightarrow \pi_a^*$ character. Conversely, the $\pi \rightarrow \pi_b^*$ transition is associated with a dark state. Since the energetic sequence of the orbitals π_a^* and π_b^* varies with the substitution patterns of fluorenol, the qualitative nomenclature introduced in Figure 3 is used. In both cases the sp^2 hybridized carbons bearing the methylene bridge (C9), feature high orbital contributions,

10.1002/chem.201802390

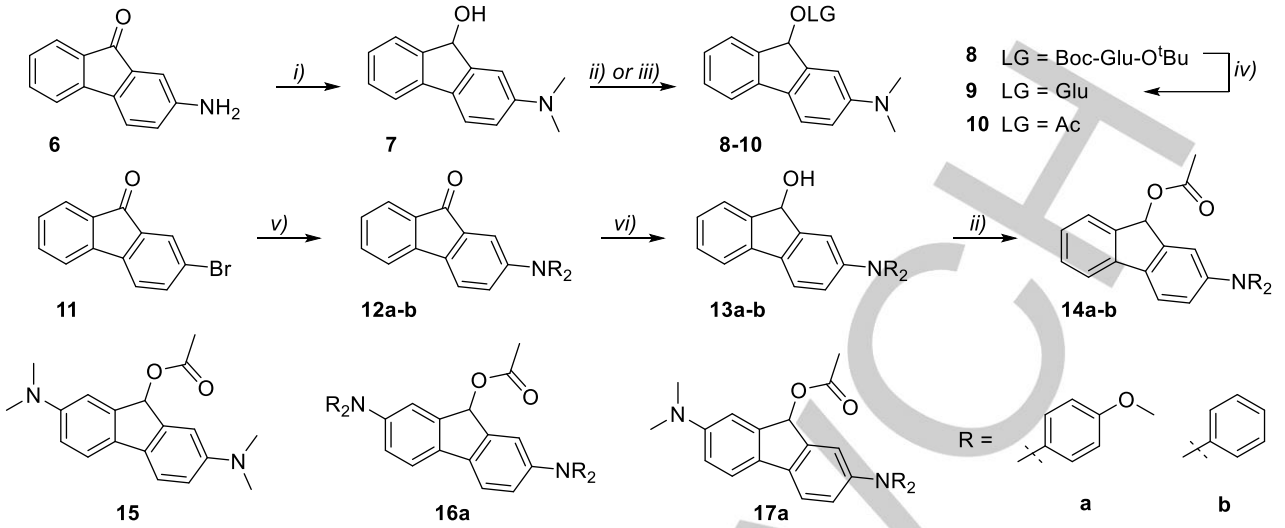

Scheme 2. Reaction sequence for the synthesis of fluorenol derivatives: *i)* H_2CO, $NaCNBH_3$, AcOH, r.t. 18 h (61%); *ii*) Ac_2O, pyridine, r.t. overnight (65% for **10**, 85% for **14a**, 50% for **14b**); *iii)* Boc-Glu-O^{t}Bu, EDC-HCl, DMAP, CH_2Cl_2. r.t. 20 h (65%); *iv)* TFA, CH_2Cl_2, r.t. 18 h (45%); *v*) HNR_2, $Pd(OAc)_2$, P^{t}Bu$_3$, toluene, 110 °C, 4-6 h (22% for **12a**, 35% for **12b**); *vi)* $NaBH_4$, THF/EtOH, r.t. 20 min (49% for **13a**, 79% for **13b**).

which is a potential prerequisite to enable photolytic cleavage of the C9-OLG bond. Computations indicated that the introduction of electron withdrawing or donating groups would result in a lower excitation energy. Introduction of electron withdrawing groups causes significant charge transfer character in the bright state, which is expected to have a negative effect on the photoactivity as in the case of the biphenyl compounds. This can be rationalized as follows: the shift of electron density in D-π-A systems is orthogonal to the direction of the bond cleavage. For this reason, electron-withdrawing groups were omitted in the fluorenol system, while in case of the second electron donating group, no clear preference for a certain position in the fluorenol ring could be determined (data not shown). Replacing of the *N*,*N*-dialkylamino with *N*,*N*-diarylamino substituent keeps its electron donating properties and further reduces the excitation energy (Table 3).

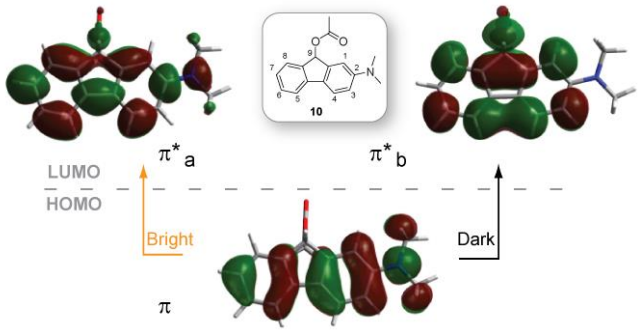

Figure 3. Molecular orbitals as obtained at the TD-PBE0/Def2-TZVP level of theory for compound **10**. The nomenclature is introduced to qualitatively account for orbital character also in related compounds. Spectroscopically dark and bright state orbital transitions are indicated accordingly.

Synthesis of the fluorenol derivatives

Based on computational results, we prepared compounds which were straightforward to derive from commercially available starting materials. To avoid additional synthetic steps of glutamic acid deprotection, we changed the leaving group to acetate. The synthesis of *N*,*N*-diarylamino fluorenols **14a-b** was started from commercially available 2-bromo-fluoren-9-one (**11**, Scheme 2, second line). The diphenylamino substituents were introduced by Buchwald-Hartwig reaction (**12a-b**), then the carbonyl group was reduced by $NaBH_4$. The resulting fluorenols **13a-b** were acylated with Ac_2O to give **14a-b**.

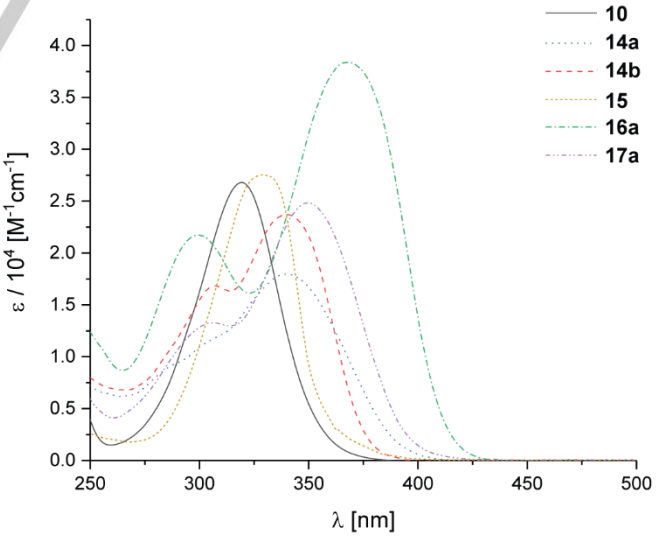

Figure 4. Molar absorption coefficients of fluorenol derivatives. Measurements were done in MeCN with 10% 0.1M TEAA buffer.

Table 3. Photochemical properties of fluorenol derivatives.

	Computational data[a]						Experimental data[b]				
Compd.	Excitation energy (nm)	S_1 Oscillator strength	Orbital transition	Excitation energy (nm)	S_2 Oscillator Strength	Orbital transition	λ_{max}[c] (nm)	$\varepsilon\lambda_{max}$ (M^{-1} cm^{-1})	ε_{365} (M^{-1} cm^{-1})	Φ_{365} (%)	$\varepsilon\Phi_{365}$[d] (M^{-1} cm^{-1})
9	n.d.[e]	n.d.	n.d.	n.d.	n.d.	n.d.	311[f]	24150[f]	1190[f]	23[f]	274[f]
10	325	0.0076	0.163 $\pi \rightarrow \pi^*_a$ 0.676 $\pi \rightarrow \pi^*_b$	305	0.5862	0.677 $\pi \rightarrow \pi^*_a$ -0.155 $\pi \rightarrow \pi^*_b$	319	26805	1160	15	174
14a	371	0.0358	-0.178 $\pi \rightarrow \pi^*_a$ 0.666 $\pi \rightarrow \pi^*_b$	365	0.5724	0.675 $\pi \rightarrow \pi^*_a$ 0.182 $\pi \rightarrow \pi^*_b$	340	17974	11069	19	2103
14b	365	0.5438	0.688 $\pi \rightarrow \pi^*_a$ 0.123 $\pi \rightarrow \pi^*_b$	351	0.0337	-0.121 $\pi \rightarrow \pi^*_a$ 0.667 $\pi \rightarrow \pi^*_b$	339	23729	9077	2.7	245
15	355	0.0001	0.085 $\pi \rightarrow \pi^*_a$ 0.694 $\pi \rightarrow \pi^*_b$	315	0.8694	0.694 $\pi \rightarrow \pi^*_a$ -0.079 $\pi \rightarrow \pi^*_b$	329	27523	2635	**42**	1107
16a	399	0.0185	-0.227 $\pi \rightarrow \pi^*_a$ 0.651 $\pi \rightarrow \pi^*_b$	394	1.1145	0.658 $\pi \rightarrow \pi^*_a$ 0.233 $\pi \rightarrow \pi^*_b$	369	38359	38201	10	3820
17a	387	0.0069	0.170 $\pi \rightarrow \pi^*_a$ 0.673 $\pi \rightarrow \pi^*_b$	365	0.8194	0.676 $\pi \rightarrow \pi^*_a$ -0.161 $\pi \rightarrow \pi^*_b$	349	24848	19702	27	**5320**

[a] Obtained TD-PBE0/Def2-TZVP level of theory. [b] Measurement were done in MeCN with 10% 0.1M TEAA buffer. [c] The value of the longest wavelength absorbance band (S_0-S_1 transition). [d] Uncaging cross section. [e] Not determined. [f] Measurement was done in 0.1M TEAA buffer with 20% MeCN.

We also prepared bis(*N*,*N*-dialkyl and diarylamino)-substituted derivatives **15, 16a** and **17a** (Scheme 2, third line). The synthetic details of these compounds can be found in the Supporting Information.

Photochemical characterisation of the fluorenol derivatives

Upon replacement of the glutamic acid leaving group with acetate, the solubility of the fluorenol photocages in aqueous solvents decreases. Therefore, we increased the amount of MeCN used for the measurements. For caging highly water-soluble compounds such as DNA or RNA, such solubility concerns are not an issue. For other substrates, polar substituents on the amino group have been shown to be effective for coumarins.[45]

The absorbance maximum of fluorenol acetate **10** is located at 319 nm (Figure 4; Table 3) and has a molar absorption coefficient of 26 805 (M^{-1} cm^{-1}). Just as in the case of the glutamic acid ester **9**, irradiation of the compound **10** as the major photoproduct produces the alcohol **7** (Fig. S13 Supporting Information). The dark hydrolysis of the fluorenol acetate **10** is slower (<1 % in 5 h) than for the fluorenol glutamate **9** probably due to the decreased amount of water in the solvent mixture, however the influence of the leaving group cannot be excluded. Replacing the methyl groups by aryl groups (**14a-b**) shifts the absorbance spectrum to longer wavelengths by 20 nm and decreases the molar absorption coefficients at the absorbance maximum. However, the molar absorption coefficients at the irradiation wavelength (365 nm) increase. The uncaging quantum yield decreases from 15% to 3% if methyl groups on nitrogen (**10**) are replaced by Ph (**14b**). This is not surprising because the *N*,*N*-diphenylamino is a poorer π-donor than *N*,*N*-dimethylamino group, due to sterical effects imposed by the phenyl groups. According to our computations the nitrogen-bearing methyl substituents are sp^2 hybridized but if methyl groups are replaced by phenyl substituents, the nitrogen atom has sp^3 character and its π-donating strength decreases. If the phenyl groups contain a 4-CH_3O substituent (**14a**), the quantum yield again increases (Φ_{365} = 19%). This is due to the increased electron donating strength of *para* methoxy substituted phenyl group when compared to unsubstituted phenyl.[46] Symmetrical dimethylamino substitution (**15**) redshifts the absorbance maximum by 10 nm (λ_{max} = 329 nm) and increases the uncaging quantum yield by nearly a factor of three (Φ_{365} = 42%) when compared to the monosubstituted analogue **10**. The structurally similar 2,7-dimetoxyfluorenol released acetate with 21% quantum yield (at 300 nm).[42] This shows that also for fluorene-derived photocages amino substituents increase the reaction quantum yields and shift the absorbance spectrum to longer wavelengths when compared to their methoxy analogues. Similar behavior has been shown for DEACM (7-*N*,*N*-diethylamino coumarin) and DEAMb photocages.[26,47] Just like compound **15** had more redshifted absorbance in comparison to monosubstitued **10**, also in the case of phenyl substitution the symmetric compound **16a** has an increased molar absorption coefficients in comparison to its unsymmetrical analogue **14a**.

However, the photoreaction's quantum yield decreases. The reason for that could be the increased likelihood of internal conversion facilitated by freely rotating aryl substituents on the amino group. Combining the best tested substitution patterns, the unsymmetrical 2,7-substituted fluorenol **17a** was prepared. The absorbance maximum of this molecule lies at 349 nm and has a high molar absorption coefficient (24 848 M^{-1} cm^{-1}). The uncaging quantum yield is 27% (Φ_{365}), thus resulting in the highest uncaging cross section ($\varepsilon\Phi_{365}$ = 5320 M^{-1} cm^{-1}) among all studied molecules.[48] Photocages with uncaging cross sections around 200 (M^{-1} cm^{-1}) have been successfully used in biological applications.[49,50] Even the least efficient fluorenol-based photocages reported in this study have an uncaging cross section close to this value (**10** $\varepsilon\Phi_{365}$ = 171, **14b** $\varepsilon\Phi_{365}$ = 244), while all other have uncaging cross sections in the range of 1000-5000 (M^{-1} cm^{-1}). These results make the reported fluorene derivatives a promising alternative to other commonly used photolabile protecting groups.

Conclusions

Introduction of a second aromatic ring can improve the spectral and photochemical properties of the 3-diethylamino benzyl (DEAMb) photolabile protecting group. However, only electron-donating substituents can be used, because electron-withdrawing substituents are detrimental to the photoactivity. These observations are in line with Zimmerman's meta effect and we could qualitatively confirm them by TDDFT computations. The molar absorption coefficients of aryl substituted DEAMb derivatives depend on the biphenyl torsion angle. The more both aromatic rings are forced out of co-planarity, the smaller the π orbitals' overlap and thereby the molar absorption coefficients. A DEAMb derivative with a phenyl substituent in *meta* position (relative to NEt_2, **3a**) was the best performing photocage from biphenyls reported in this study. Its uncaging quantum yield at 365 nm was 42%, which is enhanced compared to the reported uncaging quantum yields of *meta*-unsubstituted analogues at smaller wavelengths. Thus, we have successfully remedied one of the major drawbacks of previously reported DEAMb photocages, namely irradiation in the far UV region without losing photoactivity. In order to further improve the molar absorption coefficients of DEAMb derivatives, a rigid linker was introduced. We chose to link both aromatic rings through the benzylic carbon, resulting in fluorene derivatives. It could be shown that spectral properties of *meta*-amino substituted fluoren-9-ols are superior to DEAMb derived biphenyls and the good uncaging quantum yields shown by selected biphenyls are preserved. Photochemical properties (*e.g.* absorbance maximum, uncaging quantum yield) of these fluorene derivatives can easily be tuned by changing the amino group substituents. The fluorene-derived PPGs shown in this study also have better photochemical properties (absorbance in visible spectral range, higher quantum yields) than the fluorene derivatives known from literature. For example, 2-*N*,*N*-dimethylamino-7-*N*,*N*-di(4´-metoxyphenyl) fluorenol acetate (**17a**) demonstrates an uncaging cross section larger than 5000 M^{-1} cm^{-1} ($\varepsilon\Phi_{365}$) but its absorbance bands extends almost to the visible spectral range. These results make the reported fluorene derivatives a good alternative to other commonly used photolabile protecting groups. Further investigations about *meta*-amino substituted fluorene derivatives photochemical properties are underway.

Experimental Section

Molar absorption coefficients: All spectra were measured in 1.0 cm quartz fluorescence cuvette (QS) from *Hellma-Analytics*. Samples were prepared by weighting small amount (1-2 mg) in a glass vial, dissolved in selected binary solvent mixture and then used for preparation of dilution series. Usually 4-7 different concentrations were prepared. The UV-vis absorbance spectra of each concentration were measured. The slope of absorbance increase upon concentration increase was calculated at each wavelength. More details about molar absorption coefficient measurements can be found in the Supporting Information.

Quantum yields: 365 nm LED (M365L2, *Thorlabs*) was used as a light source. It was calibrated using actinometry (Iron (III) ferrioxalate).[51] The sample was prepared in the same solvent mixture as used for molar absorption coefficients determination. Internal standard (phenylalanine) was added and the solution was filtrated. The concentration of the photocage was determined spectroscopically. The samples were irradiated for a defined time and the reaction progress was analysed with HPLC. On average 8 different irradiation times were performed and each irradiation time was repeated 3 times. More details about quantum yield measurements can be found in the Supporting Information

Organic synthesis: All reagents and solvents were purchased from commercial sources and used as received. For normal phase column chromatography *Macherey-Nagel* silica gel 60 (particle size 0.04-0.06 mm) was used. For reverse phase column chromatography *Macherey-Nagel* prefilled Chromabond® Flash RS200 C18ec columns were used. NMR spectra were measured on a *Bruker* instrument. Spectra were referenced to the residual solvent peak in deuterated solvent: $CDCl_3$ ^1H 7.26, ^{13}C 77.16; DMSO-d_6 ^1H 2.50, ^{13}C 39.52; CD_3OD-d_4 ^1H 3.31, ^{13}C 49.00; D_2O ^1H 4.79, ^{13}C no reference was done. HRMS - High-Resolution Mass Spectrometry spectra were measured on MALDI-LTQ Orbitrap XL™ from *Thermo Fisher Scientific*. For high-performance liquid chromatography *Agilent Technologies* 1260 Infinity instrument was used and MultoKrom® 100-5 C18 column (250 x 4.6 mm) from *CS-Chromatographie Service GmbH*. The examples of synthetic procedures for selected key compounds are given in the following text. Synthetic details about other compounds can be found in the Supporting Information.[26,52–57]

General procedure A – Steglich-type esterification: Synthesis of 5-(diethylamino)-2-iodophenyl methanol Boc-O^{t}Bu-Glu ester P2 (X = *para*-I). 5-Diethylamino-2-iodobenzyl alcohol (10.0 g, 32.8 mmol, 1.0 eq) was dissolved in CH_2Cl_2 (100 mL). To the solution EDC-HCl (10.0 g, 52.3 mmol, 1.6 eq), DIPEA (5.07 g, 39.3 mmol, 1.2 eq), DMAP (0.4 g, 3.3 mmol, 0.1 eq) and *N*-(*tert*-butoxycarbonyl)-*L*-glutamic acid 1-*tert*-butyl ester (15.0 g, 49.5 mmol, 1.5 eq) was added. The reaction mixture was stirred until TLC analysis showed full conversion (20 h). Upon completion, the mixture was washed two times with 0.01M HCl, then twice with saturated $NaHCO_3$ and twice with brine. Organic layer dried over Na_2SO_4 and after filtration concentrated in reduced pressure to give slightly brown oil. After column chromatography (SiO_2, cyclohexane : ethyl acetate 5:1) the product (16.0 g, 83%) was obtained as light brown oil which upon storage becomes solid. ^1H NMR (500 MHz, $CDCl_3$): δ 7.56 (d, 1H, *J* = 8.8 Hz), 6.69 (d, 1H, *J* = 3.1

Hz), 6.37 (dd, 1H, *J* = 8.8, 3.1 Hz), 5.12-5.03 (m, 2.9H, major rotamer), 4.86-4.73 (m, 0.1H, minor rotamer), 4.26-4.17 (m, 0.9H, major rotamer), 4.12-4.01 (m, 0.1H, minor rotamer), 3.32 (q, 4H, *J* = 7.1 Hz), 2.55-2.38 (m, 2H), 2.24-2.14 (m, 1H), 2.01-1.90 (m, 1H), 1.45 (9H, s), 1.43 (9H, s), 1.14 (t, 6H, *J* = 7.1 Hz) ppm. ^{13}C NMR (125 MHz, $CDCl_3$): δ 172.6, 171.5, 155.5, 148.0, 139.8, 138.4, 113.8, 113.8, 82.3, 79.9, 79.8, 70.9, 53.5, 44.5, 30.5, 28.5, 28.3, 28.1, 12.5 ppm. HRMS (MALDI) m/z: $[M]^{\cdot+}$ Calcd for $C_{25}H_{39}IN_2O_6$ 590.18473; Found 590.18292.

General procedure B – Suzuki coupling: Synthesis of 5-(diethylamino)-2-(*para*-cyanophenyl) methanol Boc-O^{t}Bu-Glu ester P3. The reaction conditions were adopted from the literature.[58] The 5-(diethylamino)-2-iodophenyl methanol Boc-O^{t}Bu-Glu ester (*para*-iodo **P2**) (400 mg, 0.68 mmol, 1.0 eq) was dissolved in toluene (10 mL). Then 2M Na_2CO_3 (1.2 mL) was added and solution degassed by passing through argon stream for 10 min. Then $Pd(PPh_3)_4$ (47mg, 0.04 mmol, 0.06eq) was added and degassing with argon stream was repeated. In a separate flask 4-cyanobenzeneboronic acid (208 mg, 1.42 mmol, 2.1 eq) was dissolved in EtOH and degassed with argon stream before adding it to the toluene solution. The reaction mixture was then refluxed under argon atmosphere until TLC analysis showed full conversion (5 h). Upon completion the mixture was diluted with ethyl acetate and H_2O, organic phase separated, aqueous phase washed twice with ethyl acetate. The combined organic phase was washed with brine, dried over Na_2SO_4 and after filtration concentrated in reduced pressure to give slightly yellow oil. Purification was done by column chromatography (SiO_2, cyclohexane : ethyl acetate 9:1 to 3:1). However, it was not possible to separate side products (boronic acid homocoupling) in direct phase chromatography. To obtain analytically pure sample also reverse phase (C18) column chromatography was performed (MeCN : H_2O 70:30 to 100%). However, it is important to note that for next synthetic step (deprotection of *tert*-butyl and Boc esters) this impurity does not disturb and can be easily removed by filtration afterward. The product was obtained as oil (230 mg, 60%). ^{1}H NMR (500 MHz, $CDCl_3$): δ 7.68-7.64 (m, 2H), 7.45-7.42 (m, 2H), 7.13 (d, 1H, *J* = 8.6 Hz), 6.76 (d, 1H, *J* = 2.5 Hz), 6.70 (dd, 1H, *J* = 8.6, 2.5 Hz), 5.10-5.04 (m, 0.9H, major rotamer), 4.99 (s, 2H), 4.84-4.73 (m, 0.1H, minor rotamer), 4.23-4.15 (m, 0.9H, major rotamer), 4.08-3.99 (m, 0.1H, minor rotamer), 3.40 (q, 4H, *J* = 7.1 Hz), 2.47-2.30 (m, 2H), 2.18-2.08 (m, 1H), 1.92-1.83 (m, 1H), 1.45 (9H, s), 1.42 (9H, s), 1.19 (t, 6H, *J* = 7.1 Hz) ppm. ^{13}C NMR (125 MHz, $CDCl_3$): δ 172.6, 171.4, 155.5, 147.9, 145.9, 133.8, 132.1, 131.3, 130.1, 127.3, 119.2, 113.1, 111.8, 110.1, 82.4, 79.9, 65.2, 53.4, 44.5, 30.5, 28.4, 28.3, 28.1, 12.7 ppm. HRMS (MALDI) m/z: $[M^{\cdot}]^+$ Calcd for $C_{32}H_{43}N_3O_6$ 565.31464; Found 565.31301.

General procedure C – protecting group cleavage with TFA: Synthesis of 2e. The 5-(diethylamino)-2-(*para*-cyanophenyl) methanol Boc-O^{t}Bu-Glu ester **P3** (70 mg, 0.12 mmol) was dissolved in dry CH_2Cl_2 (4 mL). To the solution TFA (4 mL) was added. Resulting mixture was stirred overnight (20 h), then evaporated. Additional co-evaporation with MeCN and toluene was done to ensure that all the TFA is removed. The oily product was purified using reverse phase (C18) column chromatography (MeCN : H_2O 20:80 to 100%). After removal of the solvent, product **2e** was obtained as solid (46 mg, 73%). ^{1}H NMR (300 MHz, D_2O): δ 7.89-7.81 (m, 2H), 7.66 (d, 1H, *J* = 1.8 Hz), 7.60-7.50 (m, 4H), 5.11 (d, 2H, *J* = 2.3 Hz), 3.90 (t, 1H, *J* = 6.7 Hz), 3.67 (q, 4H, *J* = 7.2 Hz), 2.52-2.43 (m, 2H), 2.10-1.99 (m, 2H), 1.11 (t, 6H, *J* = 7.2 Hz) ppm. ^{13}C NMR (75 MHz, D_2O): δ 173.4, 171.9, 143.6, 142.6, 136.5, 135.5, 132.6, 132.2, 129.6, 123.4, 122.6, 119.3, 110.8, 64.4, 53.8, 52.3, 29.3, 24.8, 9.6 ppm. HRMS (MALDI) m/z: $[M]^+$ Calcd for $C_{23}H_{28}N_3O_4$ 410.20743; Found 410.20692.

General procedure D – reductive amination: Synthesis of 2-(dimethylamino)-9H-fluoren-9-ol (7). 2-Amino-fluoren-9-one **6** (932 mg, 4.78 mmol, 1 eq) was dissolved in AcOH (20 mL). To this mixture paraformaldehyde (890 mg, 29.6 mmol, 6.2 eq) and $NaCNBH_3$ (879 mg, 14.0 mmol, 2.9 eq) was added. The mixture was stirred overnight (18 h), then diluted with water and extracted three times with ethyl acetate. The combined organic phase washed with water, saturated $NaHCO_3$ and brine, dried over Na_2SO_4 and filtrated. The solvent was removed under reduced pressure to give light brown powder. This was crystalized from ethyl acetate and cyclohexane to give 658 mg (61%) of a slightly brown solid. ^{1}H NMR (400 MHz, $CDCl_3$): δ 7.59-7.55 (m, 1H), 7.51-7.47 (m, 2H), 7.34-7.29 (m, 1H), 7.18 (td, 1H, *J* = 7.4, 1.0 Hz), 7.04 (d, 1H, *J* = 2.4 Hz), 6.73 (dd, 1H, *J* = 8.4, 2.4 Hz), 5.51 (s, 1H), 3.02 (s, 6H) ppm. ^{13}C NMR (100 MHz, $CDCl_3$): δ 151.1, 147.5, 145.0, 141.0, 129.1, 128.7, 125.9, 125.0, 120.8, 118.7, 113.1, 109.4, 75.6, 41.0 ppm. HRMS (MALDI-LTQ Orbitrap) m/z: $[M^{\cdot}]^+$ Calcd for $C_{15}H_{15}N_1O_1$ 225.11482; Found: 225.11492.

Synthesis of 2-(dimethylamino)-9H-fluoren-9-yl Boc-O^{t}Bu-Glu ester (8): The synthesis was done according to general procedure A with small variations. Compound **7** (388 mg, 1.72 mmol, 1.0 eq) was dissolved in CH_2Cl_2 (10 mL). To the solution EDC-HCl (658 mg, 3.44 mmol, 2 eq), DMAP (21 mg, 0.17 mmol, 0.1 eq) and *N*-(*tert*-butoxycarbonyl)-L-glutamic acid 1-*tert*-butyl ester (522 mg, 1.72 mmol, 1 eq) was added. The reaction mixture was stirred until TLC analysis showed full conversion (20 h). Upon completion the mixture was diluted with CH_2Cl_2 and washed with water. The water layer was extracted two times with CH_2Cl_2. Combined organic phase was washed with brine and dried over Na_2SO_4, concentrated in reduced pressure to give slightly brown oil. After column chromatography (SiO_2, cyclohexane : ethyl acetate 9:1 to 1:1) product **9** (570 mg, 65%) was obtained as light brown oil (mixture of diastereomers). ^{1}H NMR (500 MHz, $CDCl_3$): δ 7.53-7.44 (m, 3H), 7.36-7.30 (m, 1H), 7.18-7.12 (m, 1H), 6.92 (s, 1H), 6.78-6.70 (m, 2H), 5.18-5.04 (0.9H, major rotamer), 4.90-4.75 (0.1H, minor rotamer), 4.30-4.20 (0.9H, major rotamer), 4.15-4.02 (0.1H, minor rotamer), 3.01 (s, 6H), 2.60-2.44 (m, 2H), 2.30-2.18 (m, 1H), 2.05-1.92 (m, 1H), 1.46-1.44 (m, 9H), 1.44-1.42 (m, 9H) ppm. ^{13}C NMR (125 MHz, $CDCl_3$): δ 173.9, 173.8, 171.5, 155.5, 151.0, 143.7, 143.6, 142.0, 141.3, 141.2, 129.6, 125.9, 125.8, 125.8, 120.8, 118.7, 113.3, 110.1, 82.4, 80.0, 75.7, 53.6, 53.5, 41.0, 30.7, 28.5, 28.3, 28.1 ppm. HRMS (MALDI-LTQ Orbitrap) m/z: $[M^{\cdot}]^+$ Calcd for $C_{29}H_{38}N_2O_6$ 510.27244; Found: 510.27131.

Synthesis of 2-(dimethylamino)-9H-fluoren-9-yl glutamic acid ammonium trifluoroacetate (9): The synthesis was done according to general procedure C. From compound **8** (510 mg, 1.0 mmol, 1 eq), the product (209 mg, 45%) was obtained as white powder (mixture of diastereomers). ^{1}H NMR (400 MHz, CD_3OD-d_4 + D_2O): δ 7.53-7.49 (m, 2H), 7.44 (d, 1H, *J* = 7.5 Hz), 7.34-7.29 (m, 1H), 7.15-7.09 (m, 1H), 6.97-6.94 (m, 1H), 6.79 (dd, 1H, *J* = 8.4, 2.5 Hz), 6.68 (s, 1H), 3.64 (dt, 1H, *J* = 6.3, 2.9 Hz), 2.97 (s, 6H), 2.72-2.64 (m, 2H), 2.28-2.14 (m, 2H) ppm. ^{13}C NMR (100 MHz, CD_3OD+D_2O): δ 175.0, 173.8, 152.5, 144.8, 144.7, 143.3, 143.2, 142.5, 142.5, 131.0, 130.9, 130.5, 126.8, 126.6, 121.6, 119.5, 114.7, 111.2, 76.9, 55.4, 55.4, 41.1, 31.5, 31.4, 27.7, 27.6 ppm. HRMS (MALDI-LTQ Orbitrap) m/z: $[M]^+$ Calcd for $C_{20}H_{22}N_2O_4$ 354.15796; Found: 354.15730.

General procedure E – acylation with Ac_2O: Synthesis of 2-(dimethylamino)-9H-fluoren-9-yl acetate (10): 2-Dimethylamino-9-fluorenol **7** (63 mg, 0.28 mmol, 1 eq) was dissolved in pyridine (6 mL). To the solution Ac_2O (1.08 g, 10.5 mmol, 38 eq) was added and mixture was stirred overnight. Upon completion the solution was evaporated until dryness, then purified via column chromatography (SiO_2, cyclohexane : ethyl acetate 9:1) to give 49 mg (65%) product as off white foam. ^{1}H NMR (500 MHz, $CDCl_3$): δ 7.53-7.49 (m, 2H), 7.47 (d, 1H, *J* = 7.4 Hz), 7.36-7.31 (m, 1H), 7.18-7.13 (m, 1H), 7.0-6.9 (br s, 1H), 6.81-6.69 (m, 2H), 3.01 (s, 6H), 2.19 (s, 3H) ppm. ^{13}C NMR (125 MHz, $CDCl_3$): δ 172.1, 151.0, 143.8, 142.0, 141.3, 129.8, 129.6, 125.9, 125.7, 120.9, 118.8, 113.4, 110.1, 75.5, 41.0, 21.5 ppm. HRMS (MALDI-LTQ Orbitrap) m/z: $[M^{\cdot}]^+$ Calcd for $C_{17}H_{17}NO_2$ 267.12538; Found: 267.12552.

General procedure F – Buchwald–Hartwig amination: Synthesis of 12a. 2-Bromo-9-fluorenone **11** (569 mg, 2.19 mmol, 1 eq) and 4,4′-dimethoxydiphenylamine (503 mg, 2.19 mmol, 1 eq) was dissolved in dry toluene (10 mL). To the solution was added NaO^{t}Bu (632 mg, 6.59 mmol, 3 eq) and $Pd(OAc)_2$ (24 mg, 0.11 mmol, 0.05 eq). The solution was degassed by argon stream (15 min) before addition of $P(^tBu)_3$ (44 mg, 0.21 mmol, 0.1 eq). The dark colored solution was refluxed under argon atmosphere. During reaction mixture changes colour to red. When TLC shows complete disappearance of starting material (the fluorenone), solvent was evaporated, the solid leftover dissolved in ethyl acetate and extracted with water twice. The organic layer was washed with brine, dried over Na_2SO_4, filtrated and solvent was removed under reduced pressure. Purified via column chromatography (SiO_2, cyclohexane : ethyl acetate 19:1 to 9:1 to 3:1) to collect product as dark foam (200 mg, 22%). ^{1}H NMR (400 MHz, DMSO-d_6): δ 7.60-7.57 (m, 1H), 7.56-7.48 (m, 3H), 7.25-7.20 (m, 1H), 7.14-7.07 (m, 4H), 6.99-6.94 (m, 4H), 6.90-6.83 (m, 2H), 3.76 (s, 6H) ppm. NMR data are in agreement with literature.[52]

General procedure G – reduction of carbonyl group with $NaBH_4$: Synthesis of 13a. Compound **12a** (200 mg, 0.49 mmol, 1 eq) was dissolved in THF/EtOH 1:1 mixture (5 mL) and cooled in ice bath. Then $NaBH_4$ (28 mg, 0.74 mmol, 1,5 eq) was added and the cooling bath removed. Within 20 minutes reaction mixture changes color to slightly yellow. TLC accordingly confirms complete reduction of starting material. The reaction was quenched with small amount NH_4Cl (aq. solution), solvent was evaporated, solid residue dissolved in ethyl acetate and extracted with water. The organic layer was washed with brine, dried over Na_2SO_4, filtrated and solvent was evaporated under reduced pressure. Purified via column chromatography (SiO_2, cyclohexane : ethyl acetate 19:1 to 9:1 to 3:1) to collect product as light yellow foam (98 mg, 49%). ^{1}H NMR (400 MHz, $DMSO_{D6}$): δ 7.59 (d, 1H, *J* = 7.5 Hz), 7.54 (d, 1H, *J* = 8.2 Hz), 7.48 (d, 1H, *J* = 7.4 Hz), 7.33-7.28 (m, 1H), 7.21-7.6 (m 1H), 7.06-7.02 (m, 4H), 7.00 (d, 1H, *J* = 2.2 Hz), 6.95-6.90 (m, 4H), 6.79 (dd, 1H, *J* = 8.2, 2.2 Hz), 5.72 (d, 1H, *J* = 7.3 Hz), 5.33 (d, 1H, *J* = 7.3 Hz), 3.75 (s, 6H) ppm. ^{13}C NMR (100 MHz, DMSO-d_6): δ 155.7, 148.4, 148.3, 146.4, 140.3, 139.6, 131.7, 128.3, 126.6, 126.0, 124.8, 120.5, 119.7, 118.8, 116.3, 115.0, 73.4, 55.2 ppm. HRMS (MALDI-LTQ Orbitrap) m/z: $[M^{\cdot}]^+$ Calcd for $C_{27}H_{23}NO_3$ 409.16725; Found: 409.16638.

Synthesis of 14a: Compound **14a** was prepared as described in general procedure E, using **13a** (78 mg, 0.19 mmol) as starting material. After purification (SiO_2, cyclohexane : ethyl acetate 9:1 to 3:1) 74 mg (85%) of product **14a** was obtained as a foam. ^{1}H NMR (500 MHz, DMSO-d_6): δ 7.65 (d, 1H, *J* = 7.5 Hz), 7.60 (d, 1H, *J* = 8.3 Hz), 7.45 (d, 1H, *J* = 7.5 Hz), 7.40-7.36 (m, 1H), 7.23-7.19 (m, 1H), 7.05-7.01 (m, 4H), 7.00 (d, 1H, *J* = 2.1 Hz), 6.94-6.90 (m, 4H), 6.81 (1H, dd, *J* = 8.3, 2.1 Hz), 6.57 (s, 1H), 3.74 (s, 6H), 2.07 (s, 3H) ppm. ^{13}C NMR (125 MHz, $DMSO_{D6}$): δ 171.1, 155.8, 148.6, 143.1, 141.4, 140.6, 140.1, 132.6, 129.6, 126.6, 126.6, 125.7, 121.0, 120.7, 119.3, 116.9, 115.0, 74.3, 55.2, 20.9 ppm. HRMS (MALDI-LTQ Orbitrap) m/z: $[M^{\cdot}]^+$ Calcd for $C_{29}H_{25}NO_4$ 451.17781; Found: 451.17881.

Acknowledgements

This work was supported by the Deutsche Forschungsgemeinschaft (DFG) by means of the research training group "CLiC" (GRK 1986, Complex scenarios of light-control). We thank Lennart Alsheimer, Jennifer Breitenbach and Vivien McKenney for their help. Andreas Münch, Dr. Uwe Hener, Simon Zenglein for measuring ESI, Matthias Brandl for measuring HRMS.

Keywords: Meta Effect • Photocages • Biaryls • Fluorenes • Photolysis

[1] J. Engels, E. J. Schlaeger, *J. Med. Chem.* **1977**, *20*, 907–911.
[2] J. H. Kaplan, B. Forbush, J. F. Hoffman, *Biochemistry (Mosc.)* **1978**, *17*, 1929–1935.
[3] P. Klán, T. Šolomek, C. G. Bochet, A. Blanc, R. Givens, M. Rubina, V. Popik, A. Kostikov, J. Wirz, *Chem. Rev.* **2013**, *113*, 119–191.
[4] N. Ankenbruck, T. Courtney, Y. Naro, A. Deiters, *Angew. Chem. Int. Ed.* **2018**, *57*, 2768–2798.
[5] T. Lucas, F. Schäfer, P. Müller, S. A. Eming, A. Heckel, S. Dimmeler, *Nat. Commun.* **2017**, *8*, 15162.
[6] J. Liu, J. Hemphill, S. Samanta, M. Tsang, A. Deiters, *J. Am. Chem. Soc.* **2017**, *139*, 9100–9103.
[7] H. K. Agarwal, R. Janicek, S.-H. Chi, J. W. Perry, E. Niggli, G. C. R. Ellis-Davies, *J. Am. Chem. Soc.* **2016**, *138*, 3687–3693.
[8] A. Momotake, N. Lindegger, E. Niggli, R. J. Barsotti, G. C. R. Ellis-Davies, *Nat. Methods* **2006**, *3*, 35–40.
[9] A. D. Turner, S. V. Pizzo, G. W. Rozakis, N. A. Porter, *J. Am. Chem. Soc.* **1987**, *109*, 1274–1275.
[10] N. Gagey, P. Neveu, C. Benbrahim, B. Goetz, I. Aujard, J.-B. Baudin, L. Jullien, *J. Am. Chem. Soc.* **2007**, *129*, 9986–9998.
[11] R. S. Givens, B. Matuszewski, *J. Am. Chem. Soc.* **1984**, *106*, 6860–6861.
[12] V. Hagen, J. Bendig, S. Frings, T. Eckardt, S. Helm, D. Reuter, U. B. Kaupp, *Angew. Chem. Int. Ed.* **2001**, *40*, 1045–1048.
[13] L. Fournier, I. Aujard, T. Le Saux, S. Maurin, S. Beaupierre, J.-B. Baudin, L. Jullien, *Chem. - Eur. J.* **2013**, *19*, 17494–17507.
[14] J. P. Olson, M. R. Banghart, B. L. Sabatini, G. C. R. Ellis-Davies, *J. Am. Chem. Soc.* **2013**, *135*, 15948–15954.
[15] D. J. Kunsberg, A. H. Kipping, D. E. Falvey, *Org. Lett.* **2015**, *17*, 3454–3457.
[16] D. P. Walton, D. A. Dougherty, *J. Am. Chem. Soc.* **2017**, *139*, 4655–4658.
[17] A. P. Gorka, R. R. Nani, J. Zhu, S. Mackem, M. J. Schnermann, *J. Am. Chem. Soc.* **2014**, *136*, 14153–14159.
[18] T. Šolomek, J. Wirz, P. Klán, *Acc. Chem. Res.* **2015**, *48*, 3064–3072.
[19] P. Šebej, J. Wintner, P. Müller, T. Slanina, J. Al Anshori, L. A. P. Antony, P. Klán, J. Wirz, *J. Org. Chem.* **2013**, *78*, 1833–1843.
[20] N. Umeda, H. Takahashi, M. Kamiya, T. Ueno, T. Komatsu, T. Terai, K. Hanaoka, T. Nagano, Y. Urano, *ACS Chem. Biol.* **2014**, *9*, 2242–2246.
[21] P. P. Goswami, A. Syed, C. L. Beck, T. R. Albright, K. M. Mahoney, R. Unash, E. A. Smith, A. H. Winter, *J. Am. Chem. Soc.* **2015**, *137*, 3783–3786.
[22] N. Rubinstein, P. Liu, E. W. Miller, R. Weinstain, *Chem. Commun.* **2015**, *51*, 6369–6372.
[23] T. Slanina, P. Shrestha, E. Palao, D. Kand, J. A. Peterson, A. S. Dutton, N. Rubinstein, R. Weinstain, A. H. Winter, P. Klán, *J. Am. Chem. Soc.* **2017**, *139*, 15168–15175.
[24] K. Sitkowska, B. L. Feringa, W. Szymański, *J. Org. Chem.* **2018**, *83*, 1819–1827.
[25] P. Wang, D. A. Devalankar, W. Lu, *J. Org. Chem.* **2016**, *81*, 6195–6200.
[26] P. Wang, W. Lu, D. A. Devalankar, Z. Ding, *Org. Lett.* **2015**, *17*, 2114–2117.
[27] H. E. Zimmerman, V. R. Sandel, *J. Am. Chem. Soc.* **1963**, *85*, 915–922.
[28] P. Wang, *J. Photochem. Photobiol. Chem.* **2017**, *335*, 300–310.
[29] Z. Ahmadi, J. S. McIndoe, *Chem. Commun.* **2013**, *49*, 11488–11490.
[30] F. Bureš, *RSC Adv* **2014**, *4*, 58826–58851.
[31] H. Suzuki, *Bull. Chem. Soc. Jpn.* **1959**, *32*, 1350–1356. Schematic representation of the torsion angle influence is shown in Supporting information, Figure S2.
[32] E. Riguet, C. G. Bochet, *Org. Lett.* **2007**, *9*, 5453–5456.
[33] C. Adamo, V. Barone, *J. Chem. Phys.* **1999**, *110*, 6158–6170.
[34] F. Weigend, R. Ahlrichs, *Phys. Chem. Chem. Phys.* **2005**, *7*, 3297–3305.
[35] "G09 | Gaussian.com," can be found under http://gaussian.com/glossary/g09/, **n.d.**
[36] X. Ding, P. Wang, *J. Org. Chem.* **2017**, *82*, 7309–7316.
[37] Đ. Škalamera, V. Blažek Bregović, I. Antol, C. Bohne, N. Basarić, *J. Org. Chem.* **2017**, *82*, 12554–12568.
[38] G. G. Gurzadyan, S. Steenken, *Chem. – Eur. J.* **2001**, *7*, 1808–1815.
[39] P. Wan, E. Krogh, *J. Am. Chem. Soc.* **1989**, *111*, 4887–4895.
[40] M. Rosenberg, C. Dahlstrand, K. Kilså, H. Ottosson, *Chem. Rev.* **2014**, *114*, 5379–5425.
[41] A. T. Buck, C. L. Beck, A. H. Winter, *J. Am. Chem. Soc.* **2014**, *136*, 8933–8940.

10.1002/chem.201802390

[42] A. Roxin, A. Chase, E. Jeffers, M. Lukeman, *Photochem. Photobiol. Sci.* **2011**, *10*, 920–930.
[43] K. H. Jensen, J. E. Hanson, *Chem. Mater.* **2002**, *14*, 918–923.
[44] D. Zivkovic, Investigations on 2,7-Diamino-9-Fluorenol Photochemistry, PhD Thesis, University of Basel, **2007**.
[45] V. Hagen, B. Dekowski, V. Nache, R. Schmidt, D. Geissler, D. Lorenz, J. Eichhorst, S. Keller, H. Kaneko, K. Benndorf, et al., *Angew. Chem. Int. Ed.* **2005**, *44*, 7887–7891.
[46] O. Kwon, S. Barlow, S. A. Odom, L. Beverina, N. J. Thompson, E. Zojer, J.-L. Brédas, S. R. Marder, *J. Phys. Chem. A* **2005**, *109*, 9346–9352.
[47] T. Eckardt, V. Hagen, B. Schade, R. Schmidt, C. Schweitzer, J. Bendig, *J. Org. Chem.* **2002**, *67*, 703–710.
[48] Monosubstituted fluorene derivatives (**10**, **14a-b**) upon irradiation liberates the corresponding fluorenols, while for disubstituted molecules (**15**, **16a**, **17a**) also secondary (presumably) photoproduct – the fluorenone can be seen (Fig. S14 and S15 in Supporting Information).
[49] C. Brieke, F. Rohrbach, A. Gottschalk, G. Mayer, A. Heckel, *Angew. Chem. Int. Ed.* **2012**, *51*, 8446–8476.
[50] G. C. R. Ellis-Davies, *Nat. Methods* **2007**, *4*, 619–628.
[51] C. G. Hatchard, C. A. Parker, *Proc R Soc Lond A* **1956**, *235*, 518–536.
[52] P. J. Homnick, P. M. Lahti, *Phys. Chem. Chem. Phys.* **2012**, *14*, 11961–11968.
[53] A. Zafar, R. Melendez, S. J. Geib, A. D. Hamilton, *Tetrahedron* **2002**, *58*, 683–690.
[54] T. Saitoh, S. Yoshida, J. Ichikawa, *J. Org. Chem.* **2006**, *71*, 6414–6419.
[55] C. J. Monceaux, C. Hirata-Fukae, P. C.-H. Lam, M. M. Totrov, Y. Matsuoka, P. R. Carlier, *Bioorg. Med. Chem. Lett.* **2011**, *21*, 3992–3996.
[56] K. Park, L. Tsou, A. Hamilton, *Synthesis* **2006**, 3617–3620.
[57] X. Zhang, J.-B. Han, P.-F. Li, X. Ji, Z. Zhang, *Synth. Commun.* **2009**, *39*, 3804–3815.
[58] I. Aujard, C. Benbrahim, M. Gouget, O. Ruel, J.-B. Baudin, P. Neveu, L. Jullien, *Chem. Eur. J.* **2006**, *12*, 6865–6879.

10.1002/chem.201802390

WILEY-VCH

Entry for the Table of Contents

Layout 2:

FULL PAPER

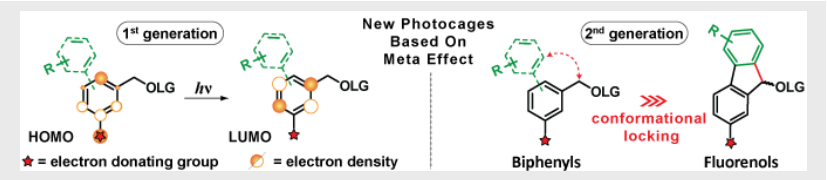

DEAMb (3-diethylaminobenzyl) photocages upon excitation undergoes electron density change in the molecule, which results in release of leaving group (Zimmerman´s meta effect). The spectral properties of DEAMb can be improved without losing its photoactivity by installing a second aromatic ring. The best improvements are achieved if a rigid fluorene system is formed by conformational locking.

Matiss Reinfelds, Jan von Cosel, Konstantin Falahati, Carsten Hamerla, Tomáš Slanina, Irene Burghardt and Alexander Heckel**

Page No. – Page No.

A new photocage derived from fluorene